Electric Power Systems Research 208 (2022) 107913

Contents lists available at ScienceDirect

Electric Power Systems Research

journal homepage: www.elsevier.com/locate/epsr

Assessing the influence of the temporal resolution on the electric vehicle charging load modeling accuracy

Toni Simolin [a,*], Kalle Rauma [b], Antti Rautiainen [a], Pertti Järventausta [a], Christian Rehtanz [b]

[a] Unit of Electrical Engineering, Tampere University, Korkeakoulunkatu 7, 33720 Tampere, Finland
[b] Institute of Energy Systems, Energy Efficiency and Energy Economics, TU Dortmund University, Emil-Figge-Str. 76, 44227 Dortmund, Germany

ARTICLE INFO

Keywords:
Charging load modeling
Electric vehicle
Hardware-in-the-loop simulation
Modeling accuracy
Temporal resolution

ABSTRACT

In the scientific literature, various temporal resolutions have been used to model electric vehicle charging loads. However, in most studies, the used temporal resolution lacks a proper justification. To provide a strengthened theoretical background for all future studies related to electric vehicle charging load modeling, this paper investigates the influence of temporal resolution in different scenarios. To ensure reliable baselines for the comparisons, hardware-in-the-loop simulations with different commercial electric vehicles are carried out. The conducted hardware-in-the-loop simulations consists of 134 real charging sessions in total. In order to compare the influence of different temporal resolutions, a simulation model is developed. The simulation model utilizes comprehensive preliminary measurement-based charging profiles that can be used to model controlled charging in fine detail. The simulation results demonstrate that the simulation model provides sufficiently accurate results in most cases with a temporal resolution of one second. Conversely, a temporal resolution of 3600 s may lead to a modeling error of 50% or even higher. Additionally, the paper shows that the necessary resolution to achieve a modeling error of 5% or less vary between 1 and 900 s depending on the scenario. However, in most cases, resolution of 60 s is reasonably accurate.

1. Introduction

In the scientific literature, it has been a common practice to model electric vehicle (EV) charging loads by using a temporal resolution of 15–60 min. However, the accuracies of different temporal resolutions are not properly analyzed. Therefore, the inaccuracies of the modeling results remain currently unknown.

When using a temporal resolution of, e.g., 60 min, the model rounds up the arrival and departure times to full hours. Additionally, only an average load of each time step can be modeled. Naturally, the coarser the resolution, the more significant the inaccuracies are likely to be. Furthermore, in case a charging control algorithm is used, the used temporal resolution of the simulation model also has an influence on the control signal. This may be a crucial factor from two points of view. Firstly, according to the charging standard IEC 61851, the minimum allowed current limit to be set by the EV supply equipment (EVSE) is 6 A which equals to 1.38 kW (230 V) in a single-phase charging point. Thus, the EVSE cannot force an EV to charge with a power of, e.g., 1 kW. Secondly, as shown in [1], EVs may not be able to use all charging currents between the minimum current limit of the EVSE (6 A) and the maximum supported charging current of the on-board charger (OBC) of the EV. By overlooking these factors, the charging load modeling may be inaccurate especially in case of controlled charging.

1.1. Related studies

The influence of temporal resolution have been assessed e.g. from a PV self-consumption point-of-view [2,3]. In [2], it is shown that the temporal resolution of the load profiles is more critical for the accuracy of the determination of self-consumption rates than the resolution of the PV generation. In [3], it is demonstrated that the error in yearly self-consumption is around 3.6%, 6.1%, 9.3%, and 12.5% when the temporal resolution is 5, 15, 30, and 60 min, respectively. According to these studies, a temporal resolution of 15 min is reasonably accurate to assess self-consumption of the PV generations. Conversely, for the optimal sizing of a battery inverter power of an energy storage system, a temporal resolution of 5 min or finer is necessary [2]. In case of modeling an uncontrolled EV charging load, these results could potentially be used as guidelines as there are no charging control signals to be considered. However, as mentioned earlier, there are two especially

* Corresponding author.
E-mail address: toni.simolin@tuni.fi (T. Simolin).

https://doi.org/10.1016/j.epsr.2022.107913
Received 19 October 2021; Received in revised form 28 February 2022; Accepted 6 March 2022
Available online 11 March 2022

Table 1.
Recent studies related to EV charging load modeling.

Refs.	T	The main objective of the study
[5]	2 h	Define Markov decision process formulation in reinforcement learning framework
[6]	1 h	Minimize charging costs and negative impacts of volatile renewable energy resource output
[7]	1 h	Voltage control through a charging pricing strategy of fast charging stations
[8]	1 h	Develop a multi-agent system to simulate energy hub with various EV penetrations
[9]	1 h	Optimize the quality of the charging service through a pricing scheme
[10]	1 h	Determine optimal EV charging stations and distributed generation units to minimize costs
[11]	1 h	Determine optimal charging stations in case of increasing EV penetration
[12]	1 h	Frequency regulation through vehicle-to-grid control while considering several uncertainties
[13]	1 h	Reduce power system generation costs through a flexible EV charge/travel schedule
[14]	30 min	Minimize EV charging costs through scheduling models
[15]	30 min	Reduce peak demand in the grid through charging scheduling
[16]	30 min	Minimize load variance and charging costs through charging behavior prediction
[17]	30 min	Propose a probabilistic approach to evaluate the impact of EVs on distribution system
[18]	15 min	Propose a spatial-temporal method to model EV charging loads in distribution network
[19]	15 min	Manage the power imbalance among feeders through tie-line voltage-source converters
[20]	15 min	Minimize peak-valley load difference through coordinated charging scheduling
[21]	15 min	Minimize charging costs and emissions with and without grid reinforcement
[22]	15 min	Reduce EV charging costs in a workplace through vehicle-to-grid control
[23]	10 min	Analyze the impacts of the EV charging load on the grid using Markov Chain simulation
[24]	5 min	Propose a data-driven approach for load modeling to guide infrastructure planning
[25]	1 min	Maximize self-consumption of photovoltaic generation via charging coordination
[26]	1 min	Present a spatial-temporal EV charging load simulation model that considers e.g. traffic
[27]	1 min	Minimize charging costs while ensuring quality of charging service
[28]	15 s	Provide centralized frequency regulation with reduced communication requirements
[29]	10 s	Coordinate EV charging loads to increase photovoltaic self-consumption

notable factors in controlled charging which may require a finer temporal resolution in order to preserve reasonable modeling accuracy.

In [4], the impact of different temporal resolutions on the peak of the normalized power (PNP) of uncontrolled EV charging is assessed. The results show that the PNP can be relatively accurately evaluated even with a resolution of 60 min when considering charging powers of 3.7 kW. When considering 22 kW charging powers, a resolution of 1 min is notably more accurate than 5 min. However, no further analyses of the impacts of the temporal resolution are conducted, and finer temporal resolutions are not considered. According to the authors' knowledge, no other studies regarding the assessment of the influence of the temporal resolution on EV charging load modeling are yet carried out.

To give an outlook of the research related to EV charging load modeling, Table 1 lists 25 recent studies. For each study, the temporal resolution (T) of the modeling is presented. Additionally, a short description of the objective of the study is shown.

As shown in Table 1, a wide range of temporal resolutions is used to model EV charging loads. In all aforementioned studies, modeling of multiple EVs were considered. Additionally, controlled charging was considered in each study except in [17–19,23,26]. However, very little effort is made to justify the selected resolutions or to assess the potential inaccuracies of the results. In [5] and [22], it is acknowledged that the temporal resolution affects the accuracy of the results. However, a further investigation is left out of the papers.

1.2. Contributions and structure

Based on the literature review, it seems necessary to assess the impacts of the temporal resolution of the EV charging load modeling. To fill the gaps in the literature, four research questions are formed:

1 *What is the impact of the temporal resolution when modeling home charging or a small charging site?* To address this question, multiple hardware-in-the-loop (HIL) simulations are carried out using 1–4 commercial EVs. The results are then compared with simulation results obtained by using different temporal resolutions (Sections 3.1 and 3.2).
2 *What is the impact of the temporal resolution when modeling a large charging site?* This question is addressed by simulating a three-month period using different temporal resolutions (Section 3.3). In this scenario, the EV charging behavior is based on real-world charging data of a commercial charging site.
3 *How accurately the EV charging loads can be modeled using the developed simulation model?* To address this question, the results of the HIL simulations are compared with the simulations results obtained by using one second temporal resolution (Section 3.5).
4 *Which temporal resolutions are necessary in different situations to ensure reasonably accurate modeling?* To address this question, the coarsest temporal resolutions that achieve a modeling error of less than 5% are presented separately for each scenario (Section 3.6).

The contribution of this paper is to carry out a thorough analysis that fills the related gap in the scientific literature and provides justified answers for the research questions. Furthermore, the goal is to provide useful guidelines and a strengthened scientific background for future studies regarding the EV charging load modeling.

The rest of the paper is as follows. Section 2 describes the assessment method. Section 3 analyses the results of each scenario. Additionally, the results are analyzed from the perspective of the overall accuracy of the simulation model, and the necessary resolutions to achieve reasonably accurate results in different scenarios are presented. The paper is finalized with conclusions in Section 4 where the research questions are addressed separately.

2. Assessment method

This section describes the used data, the key values of interest, the examined scenarios, the used control method, the experimental setup of the HIL simulations, and the used simulation model. Each part forms its own subsection.

2.1. Used data

To evaluate home charging, household electricity consumption data of a five-day period is used. The data was measured in December 2018 in one-second resolution at a detached house located in Pirkanmaa, Finland. The building is built in 2010 and its floor area is 158 m^2. A geothermal heat pump is used as the main heating system. This represents a typical new Finnish detached house. The daily energy consumption and the daily peak load varies between 34.4–59.0 kWh and 5.9–7.9 kW, respectively.

In order to evaluate a large charging site in a realistic manner, charging session data of REDI is used. REDI is a shopping center located in Helsinki, Finland, and has over 200 charging points that support 22 kW charging [30]. The data is gathered over a three-month period in 2020 (January–March) and contains 3801 charging sessions which

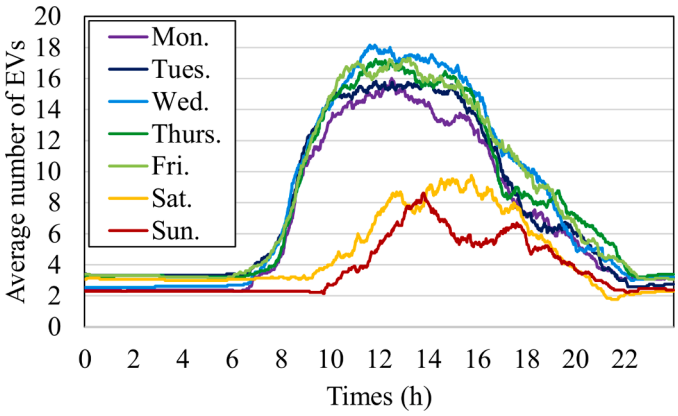

Fig. 1. The average number of EVs plugged in at REDI.

Table 2.
The used electric vehicles.

EV	Max charging power
Nissan Leaf 2012	3.7 kW (1 × 16 A)
Nissan Leaf 2019	7.4 kW (1 × 32 A)
BMW i3 2016	11.0 kW (3 × 16 A)
Smart EQ forfour 2020	22.1 kW (3 × 32 A)

Table 3
Examined scenarios.

	Site	N_{max}	N_e	Control method
S1	A household with one EV	1	45	PLM
S2	A small charging site	4	25	PLM
S3	A large charging site	21	89 [a]	Unc. / PLM

N_{max} is the maximum number of simultaneous charging sessions.
N_e is the number of different events.
[a] Scenario 3 is examined using pure simulations over an 89-day period.

results in 42.7 charging sessions per day. The data includes arrival and departure times in one second temporal resolution, charged energy, and charging peak power. According to the data, EVs have on average a stay duration of 236 min, an active charging time of 101 min, and a charged energy of 7.4 kWh. It is also seen that in 59.3% of the charging sessions the stay duration is less than 5 min longer than the active charging time. This means that the stay duration often acts as a bottleneck, and consequently, most EVs are not fully charged before departure. The average daily number of EVs plugged in at REDI is illustrated in Fig. 1.

2.2. Key values of interest

This paper aims to assess the impacts of temporal resolution in various scenarios. In order to assess the influence, three key values are examined. The key values are:

- The highest momentary peak load (P)
- The highest hourly peak load (P_h)
- The charged energy (E)

The highest momentary peak load simply refers to the highest peak load value of a single time step in a single day. The highest hourly peak load refers to the highest average loading during a one-hour long period in a single day. This is an interesting value as it can be the basis for a power-based distribution tariff component as in [31–33]. In Scenario 1, the peak loads include both the EV charging load and the household's electricity consumption. The charged energy refers to the energy that is charged during each one-hour time slot (i.e., 0:00–1:00, 1:00–2:00 etc.). This definition is made due to the selection that one hour is the coarsest temporal resolution. Furthermore, the temporal resolution in electricity pricing is often one hour and thus a modeling error in the hourly energy consumptions may affect certain cost or benefit analysis.

2.3. Examined scenarios

The simulations focus on three scenarios: (S1) a household with one EV, (S2) a small charging station with four charging points, and (S3) a large charging site with up to 21 simultaneous charging sessions. The first scenario (S1) is carried out using three EVs: Nissan Leaf 2012, Nissan Leaf 2019, and BMW i3. The home charging sessions are assumed to begin at evening. However, to generate more different circumstances, the HIL experiments are carried out using three different starting times for the charging sessions: 17:00, 19:00, and 21:00 h. A single simulated circumstance that has certain arrival time(s) and energy requirement(s) is referred to as an event. In Scenario 1, there are 45 (5 days × 3 starting times × 3 EVs) different events. To ensure more straightforward comparability, the driving distances of the EVs are kept constant at 24 km, which equals to the average daily driving distance in Finland [34]. Depending on the charging and driving efficiencies of the EVs, the energy drawn from the grid (the charging losses are included) varies between 3.5 and 6.0 kWh.

The second scenario (S2) is carried out in 25 different events. In each event, 3 or 4 of the EVs shown in Table 2 are used which results in 89 HIL charging sessions in total. For each event, the arrival times, the departure times, and the driving distances are randomly selected. In this scenario, the average driving distance is 19.1 km (distances vary between 4.3 and 65.0 km). This results in an average energy requirement of 3.8 kWh (energies vary between 0.8 and 11.6 kWh) from the grid point of view. The arrival times of the EVs varies between 16 h and 22 h and thus create circumstances where 1–4 EVs are simultaneously requesting charging. Sojourn times were assumed to be long enough so that the EVs can be fully charged.

The third scenario (S3) is formed using the charging session data of REDI. For the modeling purposes, the recorded charging peak powers are used to determine the type of the EV according to Eq. (1), where P_p is charging peak power. The third scenario is divided into three subscenarios based on the used control method: an uncontrolled charging, a peak load management (PLM) with a total charging current limit of 3 × 160 A, or a PLM with a total charging current limit of 3 × 126 A. In the case of uncontrolled charging, the highest peak current was 191 A according to the simulations. These subscenarios are used to determine the impact of the temporal resolution together with the use of charging control to the modeling accuracy in a large charging site. The control method is presented in the next subsection.

The EVs and the key parameters of the scenarios are presented in Tables 2 and 3, respectively. According to an ablation study [35], the actual EV model is not necessary attribute to model charging profiles accurately. Instead, the number of used phases and the maximum current drawn are more crucial. Therefore, as the four EVs considered in this paper have different combinations of the number of used phases and the maximum current drawn, they can be used to represent different EV fleets quite well.

$$\begin{cases} EV_{type} = Nissan\ Leaf\ 2012,\ if\ 0\ kW < P_p \leq 4.5\ kW \\ EV_{type} = Nissan\ Leaf\ 2019,\ if\ 4.5\ kW < P_p \leq 10\ kW \\ EV_{type} = BMW\ i3\ 2016,\ if\ 10\ kW < P_p \leq 15\ kW \\ EV_{type} = Smart\ EQ\ 2020,\ if\ 15\ kW < P_p \leq 25\ kW \end{cases} \quad (1)$$

It is worth mentioning that the charging data of REDI cannot be used to accurately determine the initial missing energy from the EVs. As around 60% of the EVs depart before the charging is finished, the charged energies essentially pose a lower bound for the initially missing energies of the EVs. In this paper, the charged energy in the data is assumed to be the exact energy that is initially missing from the EV when it is plugged in. This simplification means that the total charging

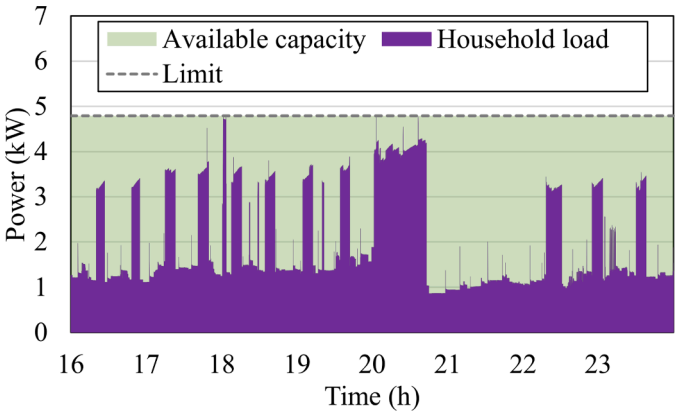

Fig. 2. Household electricity consumption and available charging capacity.

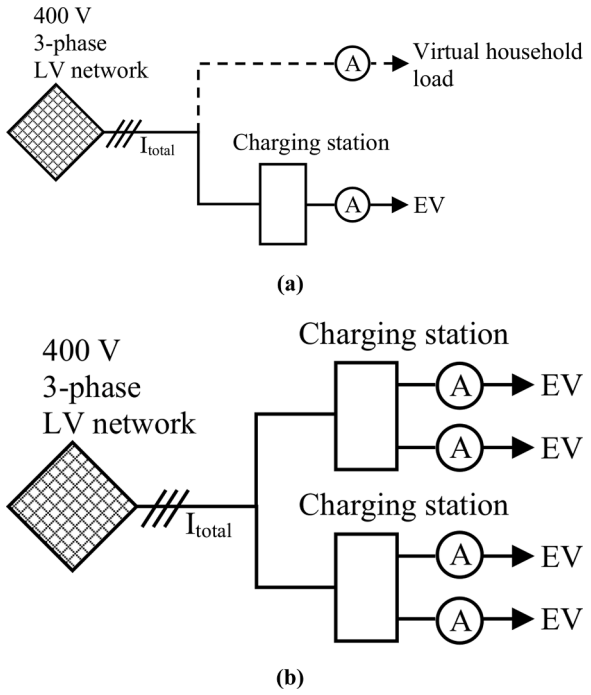

Fig. 3. The experimental setup for (a) Scenario 1 and for (b) Scenario 2.

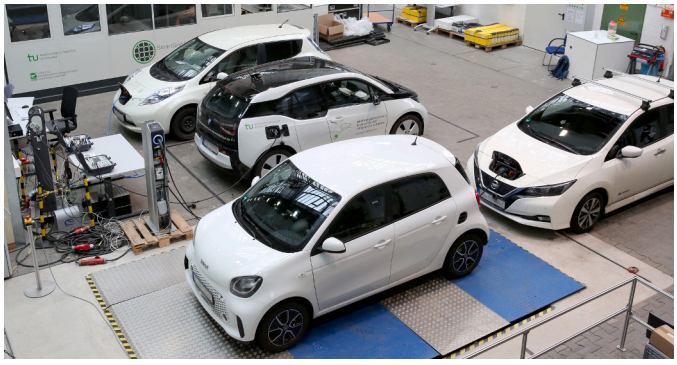

Fig. 4. The laboratory setup.

energies in the simulations are likely lower than in reality. However, the same assumption is applied for the simulations of each temporal resolution and thus the results are comparable with each other.

To form a baseline, each event in Scenarios 1 and 2 is carried out as a HIL simulation with commercial EVs. After that, the events are simulated with seven different temporal resolutions (1, 10, 30, 60, 300, 900, and 3600 s). These simulations are carried out without any HIL component. Scenario 3 is only simulated with the different temporal resolutions, and the results obtained using the temporal resolution of one second is chosen to be the baseline for this scenario. Further explanation of the experimental HIL simulation setup and the simulation model is given in Sections 2.5 and 2.6, respectively.

2.4. Control method

It is worth emphasizing that the following control method in itself is not the focus of this paper. Instead, the idea is simply to create situations where the charging currents are limited by the control system in contrast to the uncontrolled charging where the charging currents are only limited by the OBCs of the EVs. The aim of the control method is to limit peak loading. In Scenario 1, the daily load peak of the household is assumed to be known in advance and the charging power is limited so that the total load of the real estate and EV charging does not cause a higher daily load peak. An illustration of the loading of the household and the peak load limit is given in Fig. 2. In the figure, the green area between the peak load limit (gray dotted line) and the electricity consumption of the household (purple area) represents the capacity that is available for EV charging. The charging capacity for the EV can be calculated according to Eq. (2), where t is a time step, P_{max} is the highest daily peak load of the household, and $P_{household}$ is the power consumption of the household.

$$P_{EV}(t) = P_{max} - P_{household}(t). \tag{2}$$

In Scenario 2, the total loading of the charging station is limited to 3 × 32 A which allows all four charging sessions to be simultaneously active, yet a dynamic load management is required if more than one EV is charging simultaneously. In this paper, fair sharing algorithm presented in [36] is used which divides the available charging capacity evenly among the EVs. The capacity allocation is illustrated in Eq. (3) [36], where P_{EV} is the allocated power for each EV, $P_{capacity}$ is the available total charging capacity, and N is the number of active EVs requesting to be charged. Scenario 3 is essentially the same than Scenario 2 except that depending on the subscenario the total loading is either: not limited, limited to 3 × 160 A, or limited to 3 × 126 A.

$$P_{EV}(t) = \frac{P_{capacity}}{N(t)}. \tag{3}$$

As stated in the charging standard IEC 61851, an EVSE cannot set a new charging current limit for an EV more frequently than once every 5 s. Therefore, in case of HIL simulation or simulation with one-second resolution, the control algorithm is run every 5 s. In case of other resolutions, the control algorithm is run every time step.

2.5. Experimental setup

The idea of the experimental setup is to form the baselines for Scenarios 1 and 2 by measuring the real charging events. Then, the baselines are compared with the simulations. The experiments are carried out as HIL simulations at the Smart Grid Technology Lab [37] at TU Dortmund University. The hardware components include the four EVs (shown in Table 2) and two charging stations (Wirelane Doppelstele and RWE eStation). Both charging stations include two 22 kW (230 V, 3 × 32 A) sockets. The charging currents at RWE charging station are measured by using KoCoS EPPE PX power quality analyzers whereas Wirelane charging station includes built-in current measurement devices for both sockets.

The control algorithm is implemented using Python programming language. The algorithm is run on a computer that is connected to the same local network with the charging points so that the system is able to adjust the charging current limits of the EVSE and read measurements of

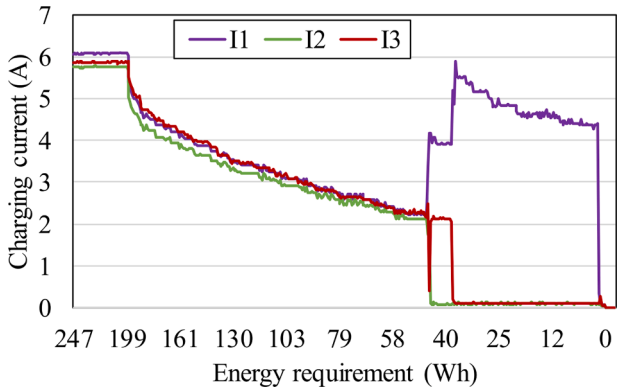

Fig. 5. Lookup table illustration of the charging of BMW i3 2016 with a current limit of 6 A, where I1–I3 represents phase currents.

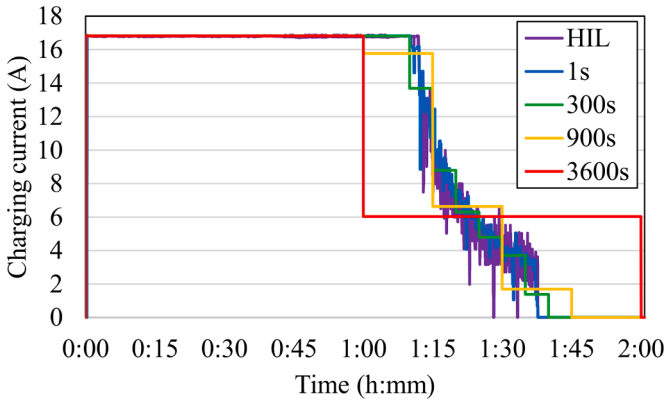

Fig. 6. Block diagram of the simulation model.

the realized charging currents in real-time. A pre-recorded household electricity consumption data (described in Section 2.1) is read from an Excel file to simulate the household electricity consumption. The experimental setups for Scenarios 1 and 2 are shown in Fig. 3. Due to the limitations of the laboratory equipment, Scenario 3 with up to 21 simultaneous charging sessions can only be simulated. The simulated setup for Scenario 3 is similar than the setup shown in Fig. 3(b) but there are 21 virtual charging points instead of the 4 physical charging points. A picture of the laboratory setup is shown in Fig. 4.

2.6. Simulation model

The idea of the simulation model is to allow the baselines of each scenario to be replicated with different temporal resolutions. These must be done as pure simulations without any HIL components. To model the EVs as accurately as possible, the modeling of the EVs is based on actual preliminary measurements of the EVs. The charging profile is measured in 1 s resolution for each EV for each possible charging current limit (integer) set by the EVSE. Only the current limit integers (6, 7, 8, … 32 A) are considered as the charging stations does not allow floating point numbers as current limits.

The preliminary measurements are used to calculate the missing energy from the batteries in each time step. The calculation begins from the end of the measurement where the missing energy is zero (i.e., the EV is fully charged). Then, a lookup table is formed to link a missing energy (Wh) to a charging current vector representing each phase current (A). The process and a formed lookup table is illustrated in Fig. 5. In the figure, the EV model is BMW i3 2016 and the current limit set by the EVSE is 6 A. A separate lookup table is formed for each EV and for each possible current limit. The lookup table is formed only for the part where

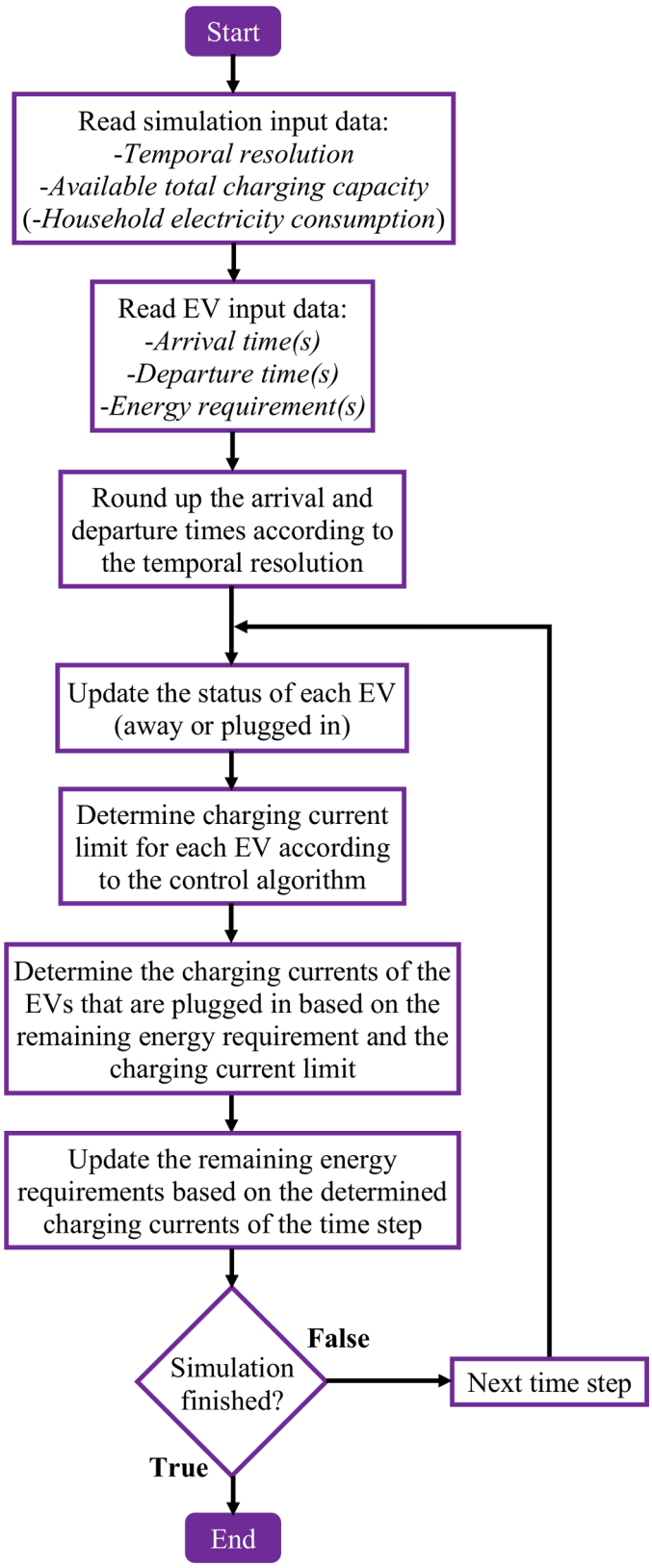

Fig. 7. Illustration of Nissan Leaf 2012 charging profile.

the charging current is decreasing. For the constant power part (e.g., energy requirement of ≥ 199 Wh in Fig. 5), the model assumes constant currents. The process and the received charging profile models are essentially the same than the ones mentioned in [38]. However, in this paper, different current limits are considered and thus the model can be

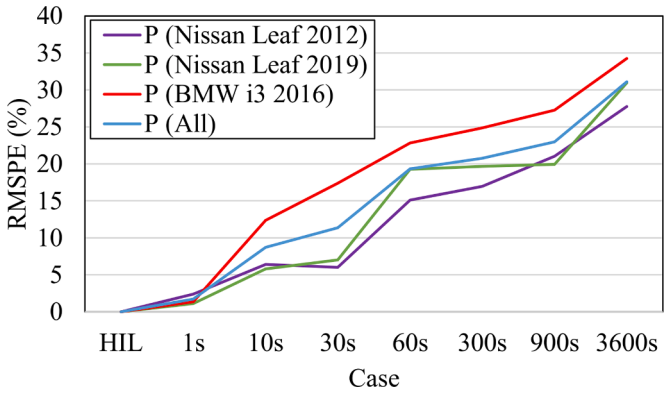

Fig. 8. RMSPE in the highest momentary peak loads in Scenario 1.

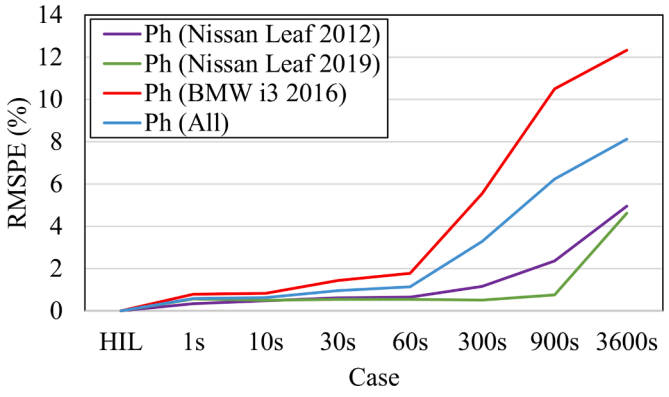

Fig. 9. RMSPE in the highest hourly peak loads in Scenario 1.

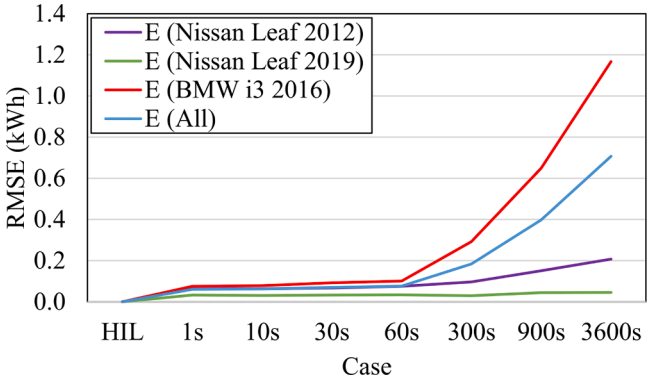

Fig. 10. RMSE in the charged energies in Scenario 1.

used to simulate controlled charging instead of only uncontrolled charging. In this paper, the energy that is missing from the battery of an EV is referred to as energy requirement.

As opposed to [38], the simulation model is modified to consider different time resolutions. Coarser time resolutions are obtained by averaging the values of the considered time period. In Fig. 6, an uncontrolled charging session of Nissan Leaf 2012 (i.e., the current limit set by the EVSE is $\geq$ 16 A) is illustrated in different cases. In the figure, "HIL" represents actual laboratory measurements whereas the rest represent simulation results with different temporal resolutions. In each of these cases, the EV draws 5.2 kWh from the grid. However, it can be clearly seen that a coarser time resolution results in a higher deviation between the measured charging profile and the simulated charging profile.

The operation of the simulation model is illustrated in Fig. 7. At the beginning, the model reads general input data and EV related input data. Since the arrivals and departures may not necessarily occur at an exact time step in all temporal resolutions, they are rounded to the closest time step. For example, an arrival time of 12:33:21 would be rounded to 12:30:00 or 13:00:00 in case of 15 min or 1 h resolutions, respectively.

After determining the initial values, the model simulates the EV charging until all EVs are fully charged or departed. In each time step, the model determines the status of each EV (away of plugged in). For the EVs that are plugged in, the charging control algorithm determines the charging current limits according to Eq. (2) or (3) depending on the scenario. After that, the charging currents are determined according to the charging profile models (lookup tables) where the realized charging currents depends on the current limits and the energy requirements. Finally, at the end of each time step, the remaining energy requirements of the EVs are updated based on the determined charging currents (assuming 230 V).

In the home charging scenario, the real-time power consumption of the household acts as a control signal for the EV charging according to Eq. (2). Even though the control is in real-time, it includes a small delay as the power consumption must be measured first before it can be used as a control signal. In the simulations, the delay is considered in case of temporal resolutions of 1–30 s. For example, in case of 30 s temporal resolution, this means that an average household power consumption of the previous 30 s period is used to determine the EV charging current limit for the next 30 s period. In case of resolutions of 60–3600 s, the delay of the real-time control is neglected as it yields more accurate results than using a delay of 60–3600 s. Therefore, for temporal resolutions of 60–3600 s, the average power consumption of a single time step is used to determine the EV charging current limit for the very same time step.

It is worth noting that minor deviation between the HIL measurements and the simulation results are expected as the simulation model does not consider factors such as battery temperatures in the modeling. It is commonly known that the battery temperature plays an important role in the EV charging and it must be considered by the battery management system to prevent dangerous situations and to maximize the performance and cycle life of battery [39]. From the power grid point of view, this can be seen, e.g., as a reduced charging current if the OBC tries to protect the battery from overheating [40]. However, due to the increased complexity of the modeling and the data requirements to form the model, the temperature factor is excluded from the simulation model.

3. Results

In this section, the results of each scenario are presented in separate subsections. In Scenarios 1–3, the results related to powers are presented as root mean square percentage errors (RMSPEs) calculated according to Eq. (4), where $\widehat{p}$ represents the baseline, p represents the compared case (i.e., simulation results obtained with different temporal resolutions), and t is a charging event (or a day in Scenario 3). As mentioned earlier, HIL measurements form the baselines in Scenario 1 and 2. Since there are not enough EVs to carry out the Scenario 3 in a similar fashion than Scenarios 1 and 2, the simulation results of the most accurate temporal resolution (1 s) are chosen to form the baseline for Scenario 3. The results related to charged energy are presented as root mean square errors (RMSEs). Percentual error related to the charged energy is assessed later in Section 3.4. Additionally, the general accuracy of the simulation model and the recommended temporal resolutions are investigated separately in Sections 3.5 and 3.6, respectively.

$$p_{RMSPE} = \sqrt{\frac{\sum_{t=1}^{T}\left(\frac{\widehat{p}_t - p_t}{\widehat{p}_t}\right)^2}{T}} \times 100\%. \quad (4)$$

To provide further values that may help future studies to select the

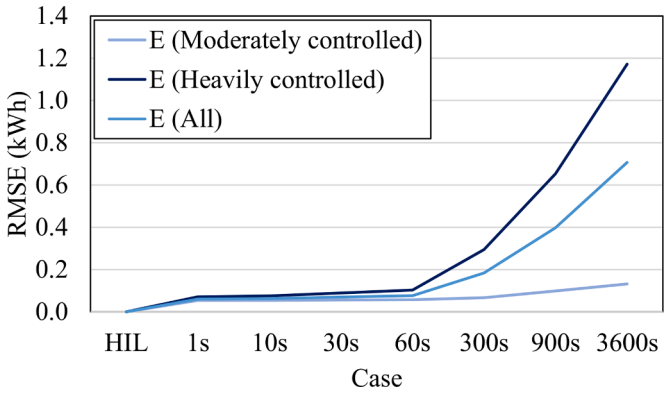

Fig. 11. RMSPE in the highest momentary peak loads in Scenario 2.

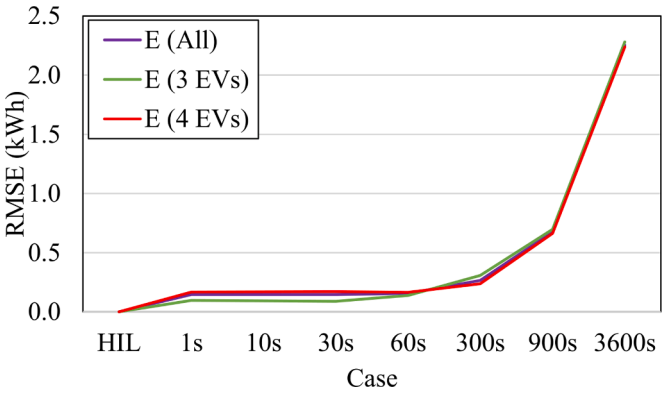

Fig. 14. RMSPE in the highest hourly peak loads in Scenario 2.

Table 4
RMSPE and RMSE for all charging events in Scenario 1.

Case	P (%)	P_h (%)	E	E[a]	E[b]
HIL	0.0	0.0	0 Wh	0 Wh	0 Wh
1s	1.7	0.6	60 Wh	53 Wh	71 Wh
10s	8.7	0.6	62 Wh	54 Wh	75 Wh
30s	19.2	0.9	69 Wh	56 Wh	89 Wh
60s	19.3	1.1	77 Wh	57 Wh	103 Wh
300s	20.8	3.3	184 Wh	66 Wh	295 Wh
900s	23.0	6.2	398 Wh	98 Wh	654 Wh
3600s	31.1	8.1	707 Wh	132 Wh	1172 Wh

[a] includes only the charging sessions that are moderately controlled.
[b] includes only the charging sessions that are heavily controlled.

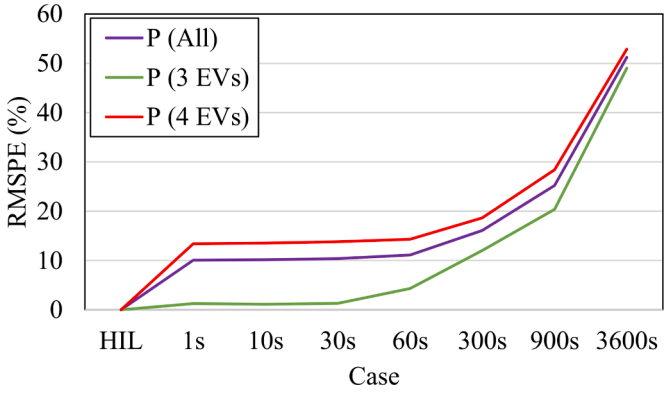

Fig. 12. RMSE in the charged energies for moderately controlled and heavily controlled charging sessions in Scenario 1.

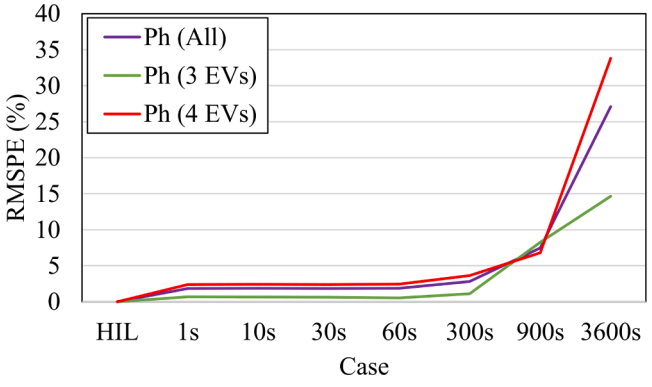

Fig. 13. RMSE in the charged energies in Scenario 2.

Table 5
RMSPE and RMSE for all charging events in Scenario 2.

Case	P	P_h	E
HIL	0.0%	0.0%	0 Wh
1s	10.1%	1.9%	145 Wh
10s	10.2%	1.9%	145 Wh
30s	10.4%	1.9%	146 Wh
60s	11.1%	1.9%	155 Wh
300s	16.1%	2.8%	265 Wh
900s	25.2%	7.5%	676 Wh
3600s	51.2%	27.1%	2254 Wh

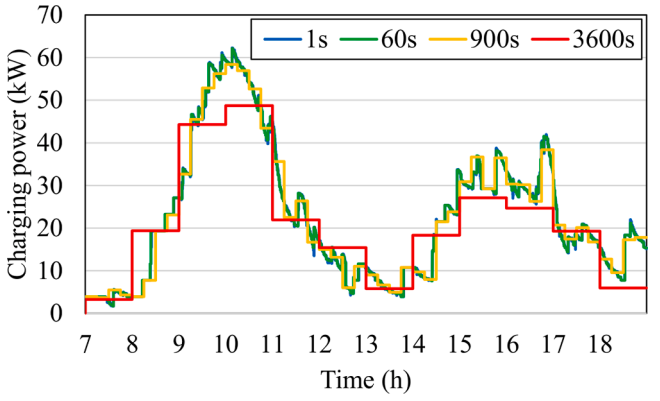

Fig. 15. Modeled charging load on 25 February 2020 in different temporal resolutions.

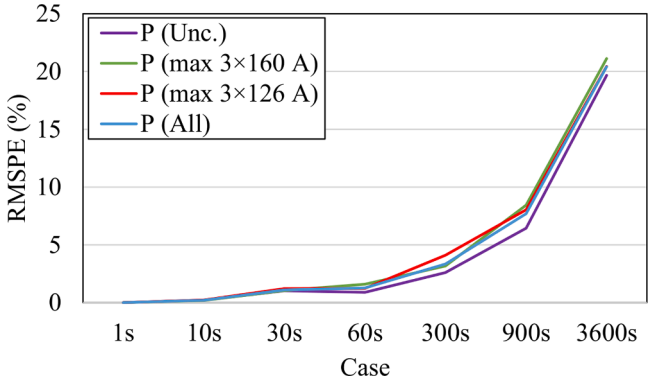

Fig. 16. RMSPE in the highest momentary peak loads in Scenario 3.

appropriate temporal resolution, mean absolute errors (MAEs) are also

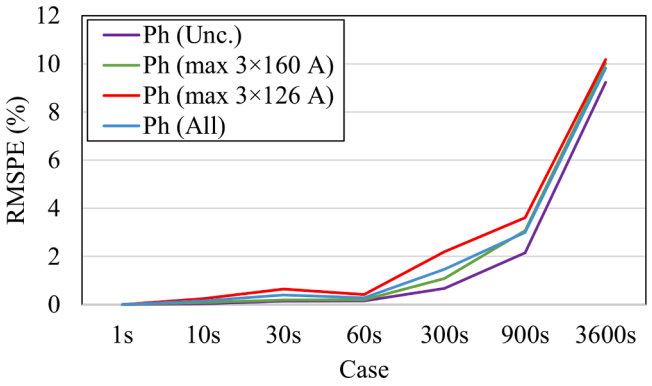

Fig. 17. RMSPE in the highest hourly peak loads in Scenario 3.

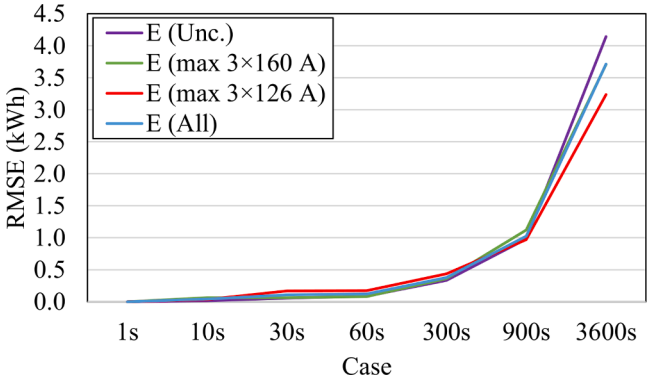

Fig. 18. RMSE in charged energies in Scenario 3.

Table 6
RMSE for all charging events in Scenario 3.

Case	P (%)	P_h (%)	E
1s	0.0	0.0	0 Wh
10s	0.2	0.2	44 Wh
30s	1.1	0.4	110 Wh
60s	1.3	0.3	121 Wh
300s	3.3	1.5	380 Wh
900s	7.7	3.0	1026 Wh
3600s	20.4	9.8	3713 Wh

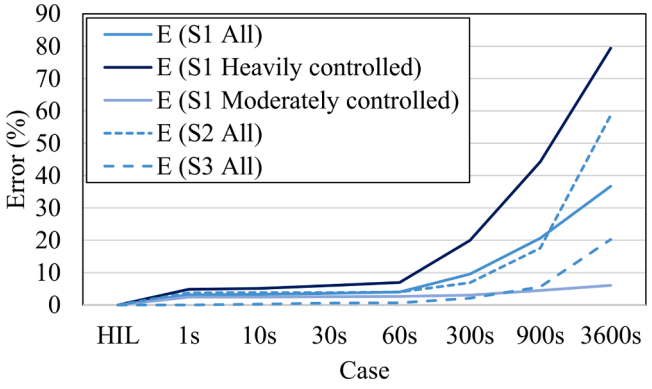

Fig. 19. Percentual error for charged energy in all scenarios.

calculated. However, to retain the flow of the paper, the MAEs are presented in the Appendix. The MAEs for Scenarios 1–3 are presented in Tables A1–A3, respectively.

Table 7
RMSE for Scenarios 1 and 2 with 1 s temporal resolution.

Scenario	P (%)	P_h (%)	E (%)
S1 (Nissan Leaf 2012)	2.4	0.3	2.8
S1 (Nissan Leaf 2019)	1.1	0.6	1.6
S1 (BMW i3 2016)	1.4	0.8	4.8
S1 (All)	1.7	0.6	3.1
S2 (3 EVs)	1.3	0.7	2.3
S2 (4 EVs)	13.4	2.4	4.3
S2 (All)	10.1	1.9	3.8

Table 8
Recommended temporal resolutions depending on the type of scenario and the considered values.

Scenario	P	P_h	E
Home charging, uncontrolled	1 s	300 s	900 s
Home charging, controlled	1 s	300 s	1 s
A small charging site, controlled	60 s [a]	300 s	60 s
A large charging site, uncontrolled	300 s [b, c]	900 s [b]	300 s [b]
A large charging site, controlled	300 s [b, c]	900 s [b]	300 s [b]

[a] In a few simulations, even a temporal resolution of 1 s resulted in an error of >10%. However, in such events, the temporal resolution of 60 s yielded results as good as the 1 s resolution. Therefore, the 60 s resolution is seen sufficient.
[b] Baseline (i.e. reference point) is the simulation result with 1 s temporal resolution instead of hardware-in-the-loop simulation.
[c] The evaluation of the simulation model indicates that the modeling of the highest momentary peak load is subject to a notable error and thus the presented temporal resolution may not be accurate.

3.1. Scenario 1: a household with one EV

In Scenario 1, the households electricity consumption acts as a control signal for the EV charging according to Eq. (2) as mentioned earlier. The results for the scenario are illustrated in Figs. 8–11. In Fig. 8, the RMSPEs in the highest momentary peak loads are presented. In the figure, it can be seen that the error is notable (5.8–12.4%) with even a temporal resolution of 10 s. For temporal resolution of 1 s and 60 s the error varies between 1.1–2.4% and 15.1–22.8%, respectively. These results were expected due to the volatile nature of the electricity consumption in households where the highest momentary peak load often lasts only for a short duration. In case of one-hour temporal resolution, the RMSPE is 27.8–34.3%. The relative errors in the highest hourly peak loads are presented for Scenario 1 in Fig. 9. When comparing Figs. 8 and 9, it can be seen that in all cases the error in the highest hourly peak loads is lower than the error in the highest momentary peak loads. Even in case of one-hour temporal resolution the error is less than 12.4%. For temporal resolutions of 60 s and 300 s the error varies between 0.5–1.8% and 0.5–5.6%, respectively.

The RMSEs in the charged energies are presented in Fig. 10. As seen in the figure, the relative error is very small (34–101 Wh) when the temporal resolution is 60 s. However, coarser resolutions tend to result in notably higher errors. In one-hour resolution, the error of all EVs is 707 Wh. By considering the fact that the average charging load of all hourly time slots in Scenario 1 where an EV is charging is 1927 Wh, the RMSE is seen considerable. A closer examination regarding the charged energy reveals a clear correlation between the magnitude of the error and the charging control. As mentioned earlier, an EVSE can adjust the charging current limit only between 6 and 80 A in charging mode 3 according to the IEC 61851 charging standard. If the available charging capacity is below 6 A, the charging must be paused until there is enough capacity available. In case of coarser temporal resolutions, more details of the household's electricity consumption are lost. And, since the household's electricity consumption is a key factor for the EV charging control in Scenario 1, coarser temporal resolutions may have notable impacts on the error of the charged energy.

In Fig. 11, the errors in the charged energies are presented separately for the charging sessions that are moderately controlled and heavily controlled. The term "moderately controlled" refers to charging sessions where the charging of the baseline did not have to be paused due to a lack of available capacity whereas the term "heavily controlled" refers to charging sessions where the charging of the baseline was paused. As seen in the figure, a finer resolution is much more important if the algorithm has to temporarily disable the charging. It is also worth noting that the IEC 61851 charging standard does not allow each phase to be controlled separately. Therefore, a three-phase charging session requires a higher minimum capacity than a single-phase charging session. This explains why the error for BMW in Fig. 10 is more heavily dependent on the temporal resolution compared to the two other EVs. The results for Scenario 1 are presented in Table 4.

It is reasonable to note that in Scenario 1, the plug-in times for the EVs were at 17:00:00, 19:00:00, or 21:00:00 and thus they were not affected by the change of the temporal resolution. Therefore, the errors seen in the results presents the influence of the temporal resolution of the control signal for a single EV. However, when modeling real-life situations, the temporal resolution is likely to affect the modeling accuracy also if the plug-in and plug-out times are rounded up by the model.

3.2. Scenario 2: a small charging site

The results of Scenario 2 are illustrated in Figs. 12–14. In Fig. 12, it can be seen that the highest momentary peak loads cannot always be accurately modeled by the simulation model even with the 1 s resolution. This means that the other assumptions and simplifications in the simulation model, such as the exclusion of considering battery temperatures, can have notable impacts to the modeling accuracy. According to a closer investigation, the simulation model was not always able to model the charging currents in the decreasing current stage correctly. This caused some charging sessions in the simulation model to finish a few minutes earlier or later than in HIL measurements. And, since the available charging capacity is divided evenly among the EVs that are requesting to be charged according to Eq. (3), a modeling error in one charging sessions can influence the charging capacity distribution if there is a charging control algorithm in use as in this scenario. As the status of the EVs are modeled wrong for only a few minutes, it does not affect the hourly peak powers or charged energies very much as it can affect the momentary peak loads as seen in Figs. 12–14. It is also worth mentioning that the issue is especially significant due to the fact that there are only a few EVs. In case of multiple EVs (as in Scenario 3), it is less impactful if, e.g., the status of one EV (requesting charging or not) is modeled wrong as it does not have relatively high influence on the total load. Conversely, if there is only one EV (as in Scenario 1), the same issue is not possible.

The above-mentioned issue occurs only in the events with four EVs, and thus, the events with three EVs are modeled more accurately especially in case of 1–60 s resolutions. For coarser resolutions ($\geq$ 300 s), the error becomes increasingly more notable and the difference between the events that have three or four EVs diminish. This is assumed to be due to the errors caused by coarse temporal resolutions become much more significant than the error caused by the other assumptions and simplifications in the simulation model excluding the temporal resolution.

The errors in the highest hourly peak loads are presented in Fig. 13. The errors seem to be relatively consistent, between 0.5–3.6%, for resolutions of 1–300 s. For resolutions of 900 s and 3600 s, the error increases to 6.8–8.3% and 14.7–33.8%, respectively. The errors in the charged energies are presented for Scenario 2 in Fig. 14. The errors for all charging events are between 145 and 155 Wh in case of temporal resolutions of 1–60 s. For coarser resolutions of 300, 900, and 3600 s, the error increases exponentially to 265, 676, and 2254 Wh, respectively. The results for Scenario 2 are presented in Table 5.

3.3. Scenario 3: a large charging site

To demonstrate the influence of different temporal resolutions in a commercial charging site, an illustration of Scenario 3 is given in Fig. 15. The day selected for the figure represents an average day in terms of daily charged energy. As seen in the figure, one-hour temporal resolution clearly results in a lower total charging power compared to other resolution. This is due to the fact that in 13.3% of the 3801 charging sessions the arrival and departure times round up to the same hour, i.e., the charging session do not essentially happen in case of one-hour resolution. In case of 900 s resolution, the arrival and departure times round up to the same moment in 3.1% of the charging sessions. In terms of energy, these charging sessions represents 3.0% (3600 s resolution) and 0.04% (900 s resolution) of the total charged energy according to the charging data.

The errors in the highest momentary peak loads in Scenario 3 is presented in Fig. 16. The figure shows that the error is relatively small ($\leq$ 1.6%) when the resolution is $\leq$ 60 s. For coarser resolutions, the error begins to increase notably. For the highest hourly peak loads, the results are similar but around half of the magnitude. The relative errors in the highest hourly peak loads are illustrated in Fig. 17. The errors in the charged energies in Scenario 3 are presented in Fig. 18. For each subscenario, the errors are $\leq$ 174 Wh for resolutions of $\leq$ 60 s. For coarser resolutions of 300, 900, and 3600 s, the errors increase exponentially to 334–436, 971–1122, and 3236–4142 kWh, respectively. The results for Scenario 3 are presented in Table 6.

3.4. Comparison of the absolute errors of the charged energies

Due to the fact that the temporal resolution affects the charged energies in each hourly time slot and may cause it to be zero in some hourly slots, the RMSPE for the charged energies were not possible to be calculated in a similar fashion than the peak loads. The RMSE in the charged energy is converted into percentual RMSE using Eq. (5), where the E_{RMSE} is the absolute RMSE (kWh) and E_{Avg} is the average hourly load of all one-hour time slots where at least one EV is charging. The results are presented in Fig. 19, where S1–S3 represents different scenarios. It can be seen that the relative error is moderately low (0.7–7.0%) in all scenarios in case of 60 s temporal resolution. In case of coarser resolutions, the error increases, but the increment is substantially dependent on the scenario.

$$E_{RMSE,\%} = \frac{E_{RMSE}}{E_{Avg}}. \tag{5}$$

3.5. Evaluating the simulation model

According to the simulation results of Scenarios 1 and 2, the simulation model successfully models the key values accurately with one second temporal resolution. The simulation results of the one-second temporal resolution are presented in Table 7. In most scenarios, the relative error in the highest momentary peak load is around 1–2%. However, the error in Scenario 2 with charging events of four EVs or all events is over 10%. As mentioned earlier, this exceptionally high error originates from the other assumptions and simplifications in the simulation model, such as the exclusion of considering battery temperatures in the modeling. Similar effect is seen also in the errors of the highest hourly peak loads. However, in all scenarios, the error in the highest hourly peak loads is much smaller compared to the errors of the highest momentary peak loads. The errors of the charged energies vary between 1.6 and 4.8% and there do not seem to be a clear trend between the scenarios and the magnitude of the error. Overall, the results indicate that the simulation model is sufficiently accurate to model the key values of the EV charging in most scenarios even though the battery temperatures are not considered in the model.

As mentioned earlier, the simulation model does not consider all

factors that influence the charging load modeling. Therefore, the simulations with different temporal resolutions include two types of modeling inaccuracies: temporal resolution-based modeling error and the errors cause by all other factors, such as the exclusion of battery temperature in the modeling. In case of a fine temporal resolution, the other factors are the dominant cause for the modeling errors whereas, in case of a coarse resolution, the temporal resolution-based inaccuracies are dominant. In Scenarios 1 and 2, the temporal resolution-based error seems to become the dominant cause of modeling errors after the temporal resolution of 60 s. This explains why the error is relatively steady for resolutions of 1–60 s and increases rapidly after resolution of 60 s in, e.g., Figs. 9–14. Additionally, as the baseline for the comparisons in Scenario 3 is the simulation results with 1 s temporal resolution instead of HIL measurements, the results include only the temporal resolution-based errors. Therefore, a more consistent correlation between the modeling errors and the temporal resolution is seen in Scenario 3 than in Scenarios 1 and 2.

3.6. Recommended temporal resolutions

As seen in the results, simplified simulations with excessively coarse temporal resolutions may lead to significant modeling inaccuracies. For example, when using one-hour temporal resolution, the error may be over 50% in the highest momentary peak loads (as seen in Fig. 12), over 30% in the highest hourly peak loads (as seen in Fig. 13), or almost 80% in the charged energies (as seen in Fig. 19). Therefore, it is clear that the use of a justified temporal resolution in simulations is vital to ensure a reasonable modeling accuracy.

In Table 8, the necessary temporal resolution to achieve a relative error of less than 5% is shown separately for each key value and for each different type of scenario. Since Scenario 3 could not be carried out as HIL simulation, the baseline is the simulation results with 1 s temporal resolution. To summarize Table 8, it can be said that to model the highest momentary peak load accurately, a fine temporal resolution of 1–60 s is necessary. To model the highest hourly peak load, a temporal resolution of 300–900 s is reasonable.

In order to model the charged energies accurately, the necessary temporal resolution vary more notable depending on the situation. If there is a volatile control signal (e.g., household's energy consumption-based control) and the charging session may be required to be temporally stopped, a very fine temporal resolution of even 1 s may be necessary. Conversely, to model the charged energy of a single EV without a complex control mechanism, a temporal resolution of 300–900 s should be sufficiently accurate. In a scenario that is between the two extremes, a temporal resolution of 60 s is likely to be reasonably accurate.

It is worth noting that this paper considers measurement-based charging load profiles in the modeling which often leads to quite accurate results as shown in Section 3.5. In case of more simplified charging load modeling approaches, the charging load modeling may contain some inaccuracies that are not related to the temporal resolution. Thus, even the use of temporal resolution of 1 s may not lead to accurate results in that case. However, by using the recommended temporal resolutions of Table 8, it is reasonable to assume that the EV charging load modeling will not include any significant temporal resolution related errors.

3.7. Discussion

The simulations of this paper consider only uncontrolled charging and controlled charging with a peak load management. It is expected that different scenarios using different control algorithms may require different temporal resolutions to be sufficiently accurate. However, all control algorithms presented in the scientific literature cannot be tested using HIL simulations with commercial EV, which sets some limitations to this kind of study. For example, the considered EVs do not support vehicle-to-grid operation and are not able to transfer information, such as battery-status, to the control system.

However, the results of this paper can also be used as guidelines for different scenarios that use other charging control algorithms. To determine the reasonably accurate temporal resolutions in case of other control algorithms, the focus should be put on the control signal and how it is affected by the change of the temporal resolution. For example, if charging is controlled based on hourly electricity prices, the control signal's resolution is an hour. Therefore, the use of one-hour resolution or finer does not negatively influence on the accuracy of the control signal. This means that charging control based solely on hourly electricity prices could be simulated with a similar accuracy as uncontrolled charging, and sufficiently accurately results could be obtained using 300–900 s resolution (see Table 8.). Furthermore, if a control algorithm combines a peak load management with a volumetric electricity price (€/kWh) optimization, the price optimization is not assumed to have an influence on the recommended temporal resolution, and thus the recommended temporal resolution is 1–300 s depending on the situation (see Table 8).

Other benchmark algorithms, such as earliest deadline first and least laxity first, may depend on the mobility requirements of the EVs including departure time or energy requirements. However, these algorithms are not expected to be notably dependent on the used temporal resolution. This is because the change of temporal resolution does not influence on the energy requirement. Additionally, the simulation model already has to consider the departure time even in the case of uncontrolled charging to determine when charging is allowed or not. A similar reasoning can potentially be used in case of other control algorithms to determine a reasonably accurate temporal resolution.

4. Conclusions

In this paper, the influence of the temporal resolution on the electric vehicle charging load modeling is assessed. To form realistic baselines for the simulations, laboratory experiments with up to four commercial electric vehicles are carried out. In addition, to evaluate electric vehicle charging at home or at a large charging site, detailed household's electricity consumption data and charging session data of REDI shopping center was used. Furthermore, a laboratory measurement–based electric vehicle charging simulation model is developed.

The investigated research questions and the findings of the study are as follows:

1 *What is the impact of the temporal resolution when modeling home charging or a small charging site?* In most cases, the modeling error is relatively modest with temporal resolutions of $\leq$ 60 s but increases exponentially with higher temporal resolutions. However, for home charging in which the peak load is the sum of the charging load and the household's electricity consumption, the modeling error is notable ($\geq$ 8.7% on average) already with temporal resolutions of $\geq$10 s.
2 *What is the impact of the temporal resolution when modeling a large charging site?* According to the results, a temporal resolution of 300–900 s may be sufficient to model the total load of a large charging site in case of uncontrolled charging or a relatively simple control method. However, it is noted that in commercial charging sites, the parking duration may not always be very long. Therefore,

exceedingly coarse resolution (e.g. one-hour) may lead to a situation where some of the charging sessions are excluded from the modeling.

3 *How accurately the electric vehicle charging loads can be modeled using the developed simulation model?* The simulation results indicate that the developed simulation model is sufficiently accurate (error less than 5%) in most cases even though the battery temperatures are not included in the model. However, the results also show that due to this simplification, there may be notable inaccuracies mostly in the highest momentary peak loads.

4 *Which temporal resolutions are necessary in different situations to ensure reasonably accurate modeling?* To model the highest hourly peak loads, a temporal resolution of 300 s is seen sufficiently accurate regardless of the size of the charging site and the use of control algorithm. To model the highest momentary peak loads in a charging site, a temporal resolution of 60–300 s is reasonably accurate. However, if the peak load is also dependent on an external load, such as a volatile household's electricity consumption, a very fine resolution of 1 s may be necessary. To model the charged energy in each hourly time slot accurately, the necessary temporal resolution varies significantly depending on the scenario. In case of uncontrolled charging of a single electric vehicle, a resolution of up to 900 s may be sufficient. However, if the charging is controlled and there is a chance that the charging must be temporally stopped (e.g. to avoid load peaks), a very fine temporal resolution of 1 s may be necessary. In other cases, a temporal resolution of 60 s is likely to be sufficiently accurate to model the charge energy.

As shown in this paper, the influence of the temporal resolution is of great importance and the use of a justified resolution should not be overlooked. To strengthen the theoretical background of all future electric vehicle charging related simulations, this paper provides guidance in terms of the necessary temporal resolution of the electric vehicle charging load modeling. Since the modeling methods and parameters play an important role in the simulations, future work should consider different EVs and investigate how different modeling methods influence on the modeling accuracy.

CRediT authorship contribution statement

Toni Simolin: Conceptualization, Software, Data curation, Formal analysis, Methodology, Validation, Visualization, Writing – original draft, Writing – review & editing. **Kalle Rauma:** Conceptualization, Data curation, Investigation, Resources, Validation, Writing – original draft, Writing – review & editing. **Antti Rautiainen:** Writing – review & editing. **Pertti Järventausta:** Writing – review & editing. **Christian Rehtanz:** Funding acquisition.

Declaration of Competing Interest

The authors declare that they have no known competing financial interests or personal relationships that could have appeared to influence the work reported in this paper.

Acknowledgments

This work was supported by the LIFE Programme of the European Union (LIFE17 IPC/FI/000002 LIFE-IP CANEMURE-FINLAND). The work reflects only the author's view, and the EASME/Commission is not responsible for any use that may be made of the information it contains. The work of Toni Simolin was supported by a grant from Emil Aaltosen Säätiö sr. Kalle Rauma would like to thank the German Federal Ministry of Transport and Digital Infrastructure for its support through the project PuLS – Parken und Laden in der Stadt (03EMF0203).

The authors would like to thank IGL Technologies for providing the charging data and TAMK for providing the household's electricity consumption data.

Appendix

Tables A1–A3.

Table A1
MAEs for Scenario 1.

Case	P	P_h	E	E[a]	E[b]
HIL	0 W	0 W	0 Wh	0 Wh	0 Wh
1s	57 W	23 W	29 Wh	30 Wh	27 Wh
10s	572 W	25 W	31 Wh	29 Wh	35 Wh
30s	694 W	36 W	41 Wh	32 Wh	57 Wh
60s	1513 W	39 W	47 Wh	38 Wh	63 Wh
300s	1660 W	86 W	106 Wh	46 Wh	210 Wh
900s	1883 W	165 W	203 Wh	66 Wh	443 Wh
3600s	2613 W	252 W	332 Wh	77 Wh	777 Wh

[a] includes only the charging sessions that are moderately controlled.
[b] includes only the charging sessions that are heavily controlled.

Table A2
MAEs for Scenario 2.

Case	P	P_h	E
HIL	0 W	0 W	0 Wh
1s	822 W	100 W	85 Wh
10s	820 W	100 W	87 Wh
30s	857 W	98 W	92 Wh
60s	975 W	97 W	103 Wh
300s	1615 W	172 W	194 Wh
900s	3371 W	462 W	506 Wh
3600s	7908 W	1323 W	1707 Wh

Table A3
MAEs for Scenario 3.

Case	P	P_h	E
1s	0 W	0 W	0 Wh
10s	41 W	19 W	11 Wh
30s	181 W	63 W	43 Wh
60s	280 W	67 W	59 Wh
300s	964 W	339 W	238 Wh
900s	2517 W	929 W	685 Wh
3600s	8891 W	3375 W	2577 Wh

References

[1] K. Rauma, T. Simolin, A. Rautiainen, P. Järventausta, C. Rehtanz, Overcoming non-idealities in electric vehicle charging management, IET Electr. Syst. Transp. (2021), https://doi.org/10.1049/els2.12025 in pressaccepted in 13 April.

[2] T. Beck, H. Kondziella, G. Huard, T. Bruckner, Assessing the influence of the temporal resolution of electrical load and PV generation profiles on self-consumption and sizing of PV-battery systems, Appl. Energy 173 (2016) 331–342, https://doi.org/10.1016/j.apenergy.2016.04.050.

[3] M. Jaszczur, Q. Hassan, A.M. Abdulateef, J. Abdulateef, Assessing the temporal load resolution effect on the photovoltaic energy flows and self-consumption, Renew. Energy 169 (2021) 1077–1090, https://doi.org/10.1016/j.renene.2021.01.076.

[4] M. Shepero, J. Munkhammar, Spatial Markov chain model for electric vehicle charging in cities using geographical information system (GIS) data, Appl. Energy 231 (2018) 1089–1099, https://doi.org/10.1016/j.apenergy.2018.09.175.

[5] N. Sadeghianpourhamami, J. Deleu, C. Develder, Definition and evaluation of model-free coordination of electrical vehicle charging with reinforcement learning, IEEE Trans. Smart Grid 11 (1) (2020) 203–214, https://doi.org/10.1109/TSG.2019.2920320.

[6] L. Gong, W. Cao, K. Liu, Y. Yu, J. Zhao, Demand responsive charging strategy of electric vehicles to mitigate the volatility of renewable energy sources, Renew. Energy 156 (2020) 665–676, https://doi.org/10.1016/j.renene.2020.04.061.

[7] X. Dong, Y. Mu, X. Xu, H. Jia, J. Wu, X. Yu, et al., A charging pricing strategy of electric vehicle fast charging stations for the voltage control of electricity distribution networks, Appl. Energy 225 (2018) 857–868, https://doi.org/10.1016/j.apenergy.2018.05.042.

[8] H. Lin, Y. Liu, Q. Sun, R. Xiong, H. Li, R. Wennersten, The impact of electric vehicle penetration and charging patterns on the management of energy hub – a multi-

agent system simulation, Appl. Energy 230 (2018) 189–206, https://doi.org/10.1016/j.apenergy.2018.08.083.
[9] Y. Zhang, P. You, L. Cai, Optimal charging scheduling by pricing for EV charging station with dual charging modes, IEEE Trans. Intell. Transp. Syst. 20 (9) (2019) 3386–3396, https://doi.org/10.1109/TITS.2018.2876287.
[10] M.F. Shaaban, S. Mohamed, M. Ismail, K.A. Qaraqe, E. Serpedin, Joint planning of smart EV charging stations and DGs in eco-friendly remote hybrid microgrids, IEEE Trans. Smart Grid 10 (5) (2019) 5819–5830, https://doi.org/10.1109/tsg.2019.2891900.
[11] Y. Zhang, J. Chen, L. Cai, J. Pan, Expanding EV charging networks considering transportation pattern and power supply limit, IEEE Trans. Smart Grid 10 (6) (2019) 6332–6342, https://doi.org/10.1109/TSG.2019.2902370.
[12] H. Liu, J. Qi, J. Wang, P. Li, C. Li, H. Wei, EV dispatch control for supplementary frequency regulation considering the expectation of EV owners, IEEE Trans. Smart Grid 9 (4) (2018) 3763–3772, https://doi.org/10.1109/TSG.2016.2641481.
[13] Y. Sun, Z. Chen, Z. Li, W. Tian, M. Shahidehpour, EV charging schedule in coupled constrained networks of transportation and power system, IEEE Trans. Smart Grid 10 (5) (2018) 4706–4716, https://doi.org/10.1109/TSG.2018.2864258.
[14] K. Zhou, L. Cheng, X. Lu, L. Wen, Scheduling model of electric vehicles charging considering inconvenience and dynamic electricity prices, Appl. Energy 276 (2020), 115455, https://doi.org/10.1016/j.apenergy.2020.115455.
[15] B. Khaki, C. Chu, R. Gadh, Hierarchical distributed framework for EV charging scheduling using exchange problem, Appl. Energy 241 (2019) 461–471, https://doi.org/10.1016/j.apenergy.2019.03.008.
[16] Y.W. Chung, B. Khaki, T. Li, C. Chu, R. Gadh, Ensemble machine learning-based algorithm for electric vehicle user behavior prediction, Appl. Energy 254 (2019), 113732, https://doi.org/10.1016/j.apenergy.2019.113732.
[17] M.P. Anand, B. Bagen, A. Rajapakse, Probabilistic reliability evaluation of distribution systems considering the spatial and temporal distribution of electric vehicles, Int. J. Electr. Power Energy Syst. 117 (2020), 105609, https://doi.org/10.1016/j.ijepes.2019.105609.
[18] Y. Xiang, Z. Jiang, C. Gu, F. Teng, X. Wei, Y. Wang, Electric vehicle charging in smart grid: a spatial-temporal simulation method, Energy 189 (2019), 116221, https://doi.org/10.1016/j.energy.2019.116221.
[19] J. Su, T.T. Lie, R. Zamora, Integration of electric vehicles in distribution network considering dynamic power imbalance issue, IEEE Trans. Ind. Appl. 56 (5) (2020) 5913–5923, https://doi.org/10.1109/TIA.2020.2990106.
[20] K. Zhou, L. Cheng, L. Wen, X. Lu, T. Ding, A coordinated charging scheduling method for electric vehicles considering different charging demands, Energy 213 (2020), 118882, https://doi.org/10.1016/j.energy.2020.118882.
[21] N.B.G. Brinkel, W.L. Schram, T.A. AlSkaif, I. Lampropoulos, W.G.J.H.M. van Sark, Should we reinforce the grid? Cost and emission optimization of electric vehicle charging under different transformer limits, Appl. Energy 276 (2020), 115285, https://doi.org/10.1016/j.apenergy.2020.115285.
[22] G.R.C. Mouli, M. Kefayati, R. Baldick, P. Bauer, Integrated PV charging of EV fleet based on energy prices, V2G, and offer of reserves, IEEE Trans. Smart Grid 10 (2) (2019) 1313–1325, https://doi.org/10.1109/TSG.2017.2763683.
[23] Y. Wang, D. Infield, Markov chain Monte Carlo simulation of electric vehicle use for network integration studies, Int. J. Electr. Power Energy Syst. 99 (2018) 85–94, https://doi.org/10.1016/j.ijepes.2018.01.008.
[24] B. Wang, D. Zhao, P. Dehghanian, Y. Tian, T. Hong, Aggregated electric vehicle load modeling in large-scale electric power systems, IEEE Trans. Ind. Appl. 56 (5) (2020) 5796–5810, https://doi.org/10.1109/TIA.2020.2988019.
[25] U. Fretzen, M. Ansarin, T. Brandt, Temporal city-scale matching of solar photovoltaic generation and electric vehicle charging, Appl. Energy 282 (2021), 116160, https://doi.org/10.1016/j.apenergy.2020.116160.
[26] J. Yan, J. Zhang, Y. Liu, G. Lv, S. Han, I.E.G. Alfonzo, EV charging load simulation and forecasting considering traffic jam and weather to support the integration of renewables and EVs, Renew. Energy 159 (2020) 623–641, https://doi.org/10.1016/j.renene.2020.03.175.
[27] Z. Wei, Y. Li, Y. Zhang, L. Cai, Intelligent parking garage EV charging scheduling considering battery charging characteristic, IEEE Trans. Ind. Electron. 65 (3) (2018) 2806–2816, https://doi.org/10.1109/TIE.2017.2740834.
[28] M. Wang, Y. Mu, Q. Shi, H. Jia, F. Li, Electric vehicle aggregator modeling and control for frequency regulation considering progressive state recovery, IEEE Trans. Smart Grid 11 (5) (2020) 4176–4189, https://doi.org/10.1109/TSG.2020.2981843.
[29] H. Kikusato, Y. Fujimoto, S. Hanada, D. Isogawa, S. Yoshizawa, H. Ohashi, et al., Electric vehicle charging management using auction mechanism for reducing PV curtailment in distribution systems, IEEE Trans. Sustain. Energy 11 (3) (2020) 1394–1403, https://doi.org/10.1109/TSTE.2019.2926998.
[30] REDI, “Parking”, 2022, https://www.redi.fi/parking/?lang=en (accessed Sep. 1, 2021).
[31] Helen Electricity Network LTD, “Electricity distribution tariffs”, 2022, https://www.helensahkoverkko.fi/globalassets/hinnastot-ja-sopimusehdot/hsv—en kku/distribution_tariffs.pdf (accessed Sep. 1, 2021).
[32] Kuopion Sähköverkko Oy, “Sähkönsiirto hinnasto - Electricity distribution tariffs”, 2022, https://www.kuopionenergia.fi/wp-content/uploads/2020/07/Sähkönsiirtohinnasto-01012020.pdf (accessed Sep. 1, 2021).
[33] LE-Sähköverkko Oy, “Verkkopalveluhinnasto - Electricity service price list”, 2022, https://www.lahtienergia.fi/wp-content/uploads/2021/06/verkkopalveluhinnasto_01082019.pdf (accessed Sep. 1, 2021).
[34] Finnish Transport and Communications Agency Traficom, “Henkilöliikennetutkimus - National passenger traffic survey 2016”, 2018, https://julkaisut.vayla.fi/pdf8/lti_2018-01_henkiloliikennetutkimus_2016_web.pdf (accessed Sep. 1, 2021).
[35] O. Frendo, J. Graf, N. Gaertner, H. Stuckenschmidt, Data-driven smart charging for heterogeneous electric vehicle fleets, Energy AI 1 (2020), 100007, https://doi.org/10.1016/j.egyai.2020.100007.
[36] T. Zhang, H. Pota, C.C. Chu, R. Gadh, Real-time renewable energy incentive system for electric vehicles using prioritization and cryptocurrency, Appl. Energy 226 (2018) 582–594, https://doi.org/10.1016/j.apenergy.2018.06.025.
[37] A. Spina, K. Rauma, C. Aldejohann, M. Holt, J. Maasmann, P. Berg, et al., Smart grid technology lab - a full-scale low voltage research facility at TU dortmund university, in: Proceedings of the 110th AEIT International Annual Conference, 2018, pp. 1–6, https://doi.org/10.23919/AEIT.2018.8577378. Oct.
[38] T. Simolin, K. Rauma, R. Viri, J. Mäkinen, A. Rautiainen, P. Järventausta, Charging powers of the electric vehicle fleet: evolution and implications at commercial charging sites, Appl. Energy 303 (2021), 117651, https://doi.org/10.1016/j.apenergy.2021.117651.
[39] L.H.J. Raijmakers, D.L. Danilov, R.A. Eichel, P.H.L. Notten, A review on various temperature-indication methods for Li-ion batteries, Appl. Energy 240 (2019) 918–945, https://doi.org/10.1016/j.apenergy.2019.02.078.
[40] Z.J. Lee, D. Chang, C. Jin, G.S. Lee, R. Lee, T. Lee, et al., Large-scale adaptive electric vehicle charging, in: Proceedings of the IEEE International Conference On Communications, Control, and Computing Technologies For Smart Grids (SmartGridComm), 2018, pp. 1–7, https://doi.org/10.1109/SmartGridComm.2018.8587550. Oct.